Dynamic X-Y Crosstalk / Aliasing Errors of Multiplexing BPMs

Till Straumann, SLAC, Menlo Park, CA 94025, USA

Abstract

Multiplexing Beam Position Monitors are widely used for their simplicity and inherent drift cancellation property. These systems successively feed the signals of (typically four) RF pickups through one single detector channel. The beam position is calculated from the demultiplexed base band signal. However, as shown below, transverse beam motion results in positional aliasing errors due to the finite multiplexing frequency. Fast vertical motion, for example, can alias into an apparent, slow horizontal position change.

INTRODUCTION

Fig. 1 shows a typical arrangement of four BPM pickup electrodes or "buttons" in the cross section of a vacuum chamber. A bunched beam of charged particles travels in z-direction, inducing RF signals to the pickups. A multiplexing BPM processing system (fig. 2) sequentially samples the buttons $A..D$ using a single receiver channel. Since only amplitude ratios are needed to determine the beam position, this approach features good drift rejection.

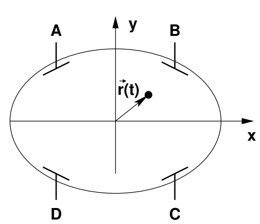

$$\begin{aligned} \tilde{a} &= (-x+y+k)I_0 \\ \tilde{b} &= (+x+y+k)I_0 \\ \tilde{c} &= (+x-y+k)I_0 \\ \tilde{d} &= (-x-y+k)I_0 \end{aligned} \qquad (1)$$

Figure 1: BPM Geometry and linear model equations

LINEAR MODEL

To the first order, the amplitudes of the pickup signals induced by a particle beam at position (x, y) can be approximated by eqns. 1 where x and y are assumed to be properly scaled according to the beam pipe geometry, and deviations from symmetry are neglected. k is a constant offset and I_0 denotes the beam current.

Note that $\tilde{a}..\tilde{d}$ actually refer to RF signal amplitudes. However, for the purpose of this analysis, we neglect the fact that a practical system (fig. 2) multiplexes RF signals into a single receiver/detector. We simply assume the presence of four identical detectors upstream of the multiplexer such that the entire analysis can be performed in base-band.

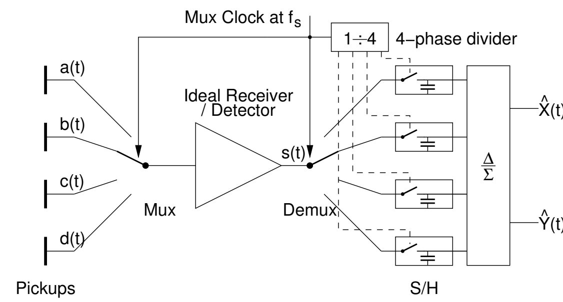

Figure 2: Multiplexing BPM system block diagram. All signals are in baseband, normalized to the beam current.

The beam position can be determined from the normalized button signals $a..d = \tilde{a}/I_0..\tilde{d}/I_0$:

$$\begin{aligned} \tilde{I}_0 &= (+\tilde{a}+\tilde{b}+\tilde{c}+\tilde{d})/4 \\ \hat{x} &= (-a+b+c-d)/4 \\ \hat{y} &= (+a+b-c-d)/4 \end{aligned}$$

We use a "$\hat{}$" accent to distinguish the system response from the "true" beam position.

DYNAMIC SYSTEM BEHAVIOR

Let's now investigate the dynamic behavior of the multiplexed BPM system running at a multiplexing clock frequency of f_s, i.e. each button gets measured at a rate of $f_s/4$. Beam motion can be described by a time dependent vector in the x, y plane.

$$\vec{r}(t) = \{x(t), y(t)\}$$

For further analysis, we assume the motion to be band-limited to $\pm f_s/2$.

Multiplexer Analysis

The time-multiplexed signal $s(t)$ consists of a stream of "excerpts" of the individual pickup signals $a(t)..d(t)$. We introduce the abbreviated notion:

$$s^{\square}(t) = \{a, b, c, d\} = \begin{cases} a(t) & 0 \leq t < T_s \\ b(t) & T_s \leq t < 2T_s \\ c(t) & 2T_s \leq t < 3T_s \\ d(t) & 3T_s \leq t < 4T_s \end{cases}$$

Besides sampling the pickups in a "(counter) clockwise" (a, b, c, d) fashion, there exists the possibility of scanning them in the "butterfly" sequence $s^{\bowtie}(t) = \{a, c, b, d\}$. (Due to symmetry, all other possible schemes are equivalent with either of the two basic ones.)

Introducing our linear model (eqns. 1)[1], we obtain

$$\begin{aligned} s^{\Box}(t) &= \left\{ \begin{array}{cccc} -x & +x & +x & -x \\ +y & +y & -y & -y \\ +k\,, & +k\,, & +k\,, & +k \end{array} \right\} \\ &= \quad x(t)\,\{-1,+1,+1,-1\} \\ &\quad + \; y(t)\,\{+1,+1,-1,-1\} \\ &\quad + \quad k \;\; \{+1,+1,+1,+1\} \end{aligned} \tag{2}$$

By rearranging the piecewise continuous function $s^{\Box}(t)$ we could decompose it into three terms, each a product of a continuous, position/time dependent function with a simple discontinuous "rectangular wave" function. In the same way, $s^{\bowtie}(t)$ can be stated:

$$\begin{aligned} s^{\bowtie}(t) = &\quad x(t)\,\{-1,+1,+1,-1\} \\ &+ \; y(t)\,\{+1,-1,+1,-1\} \\ &+ \quad k \;\; \{+1,+1,+1,+1\} \end{aligned} \tag{3}$$

The multiplexer can be seen as a *modulator*: x and y are modulated onto two ("rectangular wave") quadrature carriers at $f_s/4$ ("clockwise" multiplexing). The constant offset ("k") term remains at base-band. The "butterfly" multiplexer modulates x and y onto two carriers at $f_s/4$ and $f_s/2$, respectively. Introducing the "carrier sequences"

$$\begin{aligned} c_0(t) &= \{+1,+1,+1,+1\} && \text{"base band"} \\ c_1^i(t) &= \{-1,+1,+1,-1\} && f_s/4;\ \text{"I phase"} \\ c_1^q(t) &= \{+1,+1,-1,-1\} && f_s/4;\ \text{"Q phase"} \\ c_2(t) &= \{+1,-1,+1,-1\} && f_s/2 \end{aligned} \tag{4}$$

we rewrite eqns. 2 and 3:

$$s^{\Box}(n) = x(t)\,c_1^i(t) + y(t)\,c_1^q(t) + k \tag{5}$$

$$s^{\bowtie}(n) = x(t)\,c_1^i(t) + y(t)\,c_2(t) + k \tag{6}$$

The "carriers" defined by eqns. 4 have the properties

$$\begin{array}{rclrcl} c_i(t) * c_i(t) &=& c_0(t) & c_1^i(t) * c_1^q(t) &=& -c_2(t) \\ c_0(t) * c_i(t) &=& c_i(t) & c_1^i(t) * c_2(t) &=& -c_1^q(t) \\ && & c_1^q(t) * c_2(t) &=& -c_1^i(t) \end{array} \tag{7}$$

Frequency Domain To facilitate analysis in frequency domain, we already account for the downstream sample and hold processing and calculate the z-transform of $s^{\Box}(nT_s)$ sampled at integer multiples of the multiplexer clock period:

$$\begin{aligned} s^{\Box}(nT_s) = &\quad x(nT_s)\,(\sin(n\tfrac{\pi}{2}) - \cos(n\tfrac{\pi}{2})) \\ &+ \; y(nT_s)\,(\sin(n\tfrac{\pi}{2}) + \cos(n\tfrac{\pi}{2})) \\ &+ \; k \end{aligned} \tag{8}$$

For the sequences $c_1^i(nT_s)$ and $c_1^q(nT_s)$, adequate representations involving trigonometric functions were chosen:

$$\begin{aligned} c_1^i(nT_s) &= \sin(n\tfrac{\pi}{2}) - \cos(n\tfrac{\pi}{2}) = -\sqrt{\tfrac{j}{2}}\,j^n + \sqrt{\tfrac{-j}{2}}\,j^{-n} \\ c_1^q(nT_s) &= \sin(n\tfrac{\pi}{2}) + \cos(n\tfrac{\pi}{2}) = -\sqrt{\tfrac{-j}{2}}\,j^n + \sqrt{\tfrac{j}{2}}\,j^{-n} \\ c_2(nT_s) &= \cos(n\pi) = (-1)^n \end{aligned} \tag{9}$$

Using the correspondences [1]

$$\begin{aligned} f(nT_s) &\rightleftharpoons F(z) \\ f(nT_s)\,q^n &\rightleftharpoons F(z/q) \end{aligned} \tag{10}$$

the z-transform of eq. 8 becomes (we use lower case symbols for time domain and upper case symbols for z or frequency domain dependent variables)

$$\begin{aligned} S^{\Box}(z) = &-\sqrt{\tfrac{j}{2}}\,X(z\,\mathrm{e}^{-j\frac{\pi}{2}}) + \sqrt{\tfrac{-j}{2}}\,X(z\,\mathrm{e}^{j\frac{\pi}{2}}) \\ &-\sqrt{\tfrac{-j}{2}}\,Y(z\,\mathrm{e}^{-j\frac{\pi}{2}}) + \sqrt{\tfrac{j}{2}}\,Y(z\,\mathrm{e}^{j\frac{\pi}{2}}) + \tfrac{k}{1-z^{-1}} \end{aligned}$$

In frequency domain, the spectra $X(f)$ and $Y(f)$ (which, according to our assumption are band limited to $\pm f_s/2$,) appear shifted by an amount of $\pm f_s/4$ since

$$z\,\mathrm{e}^{\mp j\frac{\pi}{2}}\Big|_f = \mathrm{e}^{j\frac{2\pi}{T_s}f}\,\mathrm{e}^{\mp j\frac{\pi}{2}} = \mathrm{e}^{j\frac{2\pi}{T_s}(f\mp\frac{f_s}{4})} = z\big|_{f\mp\frac{f_s}{4}}$$

Again, the "mixing" behavior of the multiplexer becomes apparent: The time multiplexed signal $s(t)$ can be seen as a *frequency multiplexed* representation of the position information $\{x, y\}$ where $X(f)$ and $Y(f)$ occupy different "slots" in frequency domain. In case of the "clockwise" sampling scheme, X and Y are in fact centered around the same frequency, $\pm f_s/4$, but the complex spectra are in quadrature. The Y contribution to the "butterfly" signal $S^{\bowtie}(f)$ appears shifted by $f_s/2$ as can easily be seen by performing the z-transform with the representation $c_2(nT_s) = \cos(n\,\pi)$ according to eq. 9.

Fig. 3 sketches the X and Y spectral contributions to the multiplexed signal for "clockwise" (left) and "butterfly" (right) sampling. In the former case, X and Y appear both centered around $\pm\frac{f_s}{4}$ but with different symmetry properties with respect to the origin[2]; in the latter case, Y is shifted by $\pm\frac{f_s}{2}$ and its spectral density is doubled due to overlapping. The singular contribution of the constant term k is not shown.

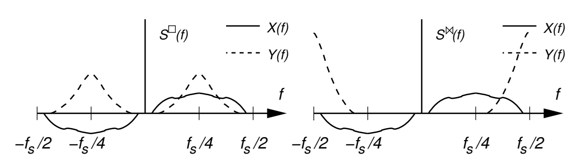

Figure 3: Multiplexed signal spectra (limited to the first Nyquist zone); "clockwise" (left) and "butterfly" (right) schemes.

Demultiplexer

The demux subsystem of fig. 2 shall be transformed into an equivalent structure which is easier to understand. Fig. 4 shows the demultiplexer and the difference network for the x channel. We begin with moving the negative coefficients

[1] The respective sums are written vertically into four columns corresponding to the four "time slots"

[2] In reality, the spectra are of course *complex* and the schematical "even"/"odd" symmetries merely should symbolize the fact that the carrier phase affects the shifted spectra's phase response such that the "composite" spectrum S still can be decomposed into X and Y contributions.

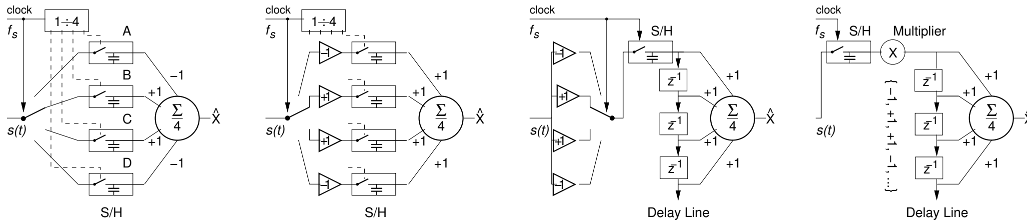

Figure 4: Transformation of the demultiplexer into an equivalent structure

upstream of the S/H circuits. This eliminates the need for "remembering" if a given S/H output has to be fed into a $-$ or $+$ input because the sign has already been accounted for. The "old" samples can then simply passed along a delay line which is fed by a single S/H running at the full multiplexer frequency f_s. Finally, – as we already know, – the multiplexer tapping off the weighted input signal can be replaced by a modulator.

Hence, the demultiplexer in combination with the difference network works as a *demodulator* translating the desired component of the composite signal $s(t)$ back to baseband. The demodulator output signals (for the moment, we neglect the averaging effect due to the delay line which is discussed below) of a "clockwise" and "butterfly" BPM are (multiplying eqns. 5 and 6 by the appropriate "carrier" and using eq. 7)

$$\begin{array}{rcccl} \hat{x}^{\square} &=& c_1^i\left(x\,c_1^i + y\,c_1^q + k\right) &=& x - y\,c_2 + k\,c_1^i \\ \hat{y}^{\square} &=& c_1^q\left(x\,c_1^i + y\,c_1^q + k\right) &=& y - x\,c_2 + k\,c_1^q \\ \hat{x}^{\bowtie} &=& c_1^i\left(x\,c_1^i + y\,c_2 + k\right) &=& x - y\,c_1^q + k\,c_1^i \\ \hat{y}^{\bowtie} &=& c_2\left(x\,c_1^i + y\,c_2 + k\right) &=& y - x\,c_1^q + k\,c_2 \end{array} \tag{11}$$

The fact that the difference network actually accumulates a "history" of four samples also becomes obvious in the transformed structure. The averaged delay line shows the typical fourth order CIC behavior ($\frac{1-z^{-4}}{1-z^{-1}}$) [2].

DISCUSSION

Eqns. 11 can be transformed to z-domain yielding e.g. for the first line (including the delay line filtering effect):

$$\begin{array}{rcl} \hat{X}^{\square}(z) &=& \left(X(z) + X_Y^{\square}(z) + k\,C_1^i(z)\right)\,H(z) \\ X_Y^{\square}(z) &=& -Y(z\mathrm{e}^{j\pi}) = -Y(-z) \\ C_1^i(z) &=& (1 + j\,z^{-1})/(1 + z^{-2}) \\ H(z) &=& (1 - z^{-4})/(1 - z^{-1}) \end{array} \tag{12}$$

In addition to the desired "X" position information, the system response contains a "crosstalk" or "alias" contribution X_Y. The constant offset k introduces a "carrier feedthrough" (as can be seen from eqns. 11 – $C_1^i(z)$ does not converge for $|z| == 1$). The "filter" response, $H(z)$, a consequence of the delay line, features zeroes at $\frac{f_s}{4}$ and $\frac{f_s}{2}$ thus effectively notching the k contribution.
Evaluating z at real frequencies, the crosstalk term becomes

$$X_Y^{\square}(f) = -Y(\mathrm{e}^{j2\pi f T_s}\mathrm{e}^{-j2\pi\frac{f_s}{2}T_s}) = -Y(f - f_s/2)$$

i.e. the Y channel feeds into $\hat{X}^{\square}$ but shifted by $\frac{f_s}{2}$. This means that e.g. a purely sinusoidal vertical beam motion $y(t) = y_0 \sin(\frac{\omega_s}{2}t)$ appears at the output $\hat{x}$ as a steady state error $\hat{x}(t) = y_0$. The analogous crosstalk contributions to $\hat{Y}^{\square}$, $\hat{X}^{\bowtie}$ and $\hat{Y}^{\bowtie}$ are

$$\begin{array}{rcl} Y_X^{\square}(f) &=& -X(f - \frac{f_s}{2}) \\ X_Y^{\bowtie}(f) &=& \sqrt{\frac{-j}{2}}\,Y(f - \frac{f_s}{4}) - \sqrt{\frac{j}{2}}\,Y(f + \frac{f_s}{4}) \\ Y_X^{\bowtie}(f) &=& \sqrt{\frac{-j}{2}}\,X(f - \frac{f_s}{4}) - \sqrt{\frac{j}{2}}\,X(f + \frac{f_s}{4}) \end{array}$$

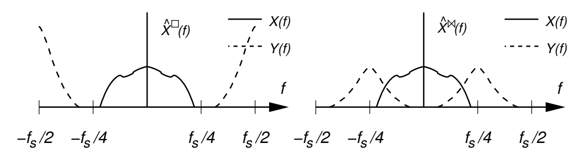

Figure 5: System frequency response (limited to the first Nyquist zone) showing y–x crosstalk for the "clockwise" (left) and "butterfly" (right) schemes.

Note that although from looking at fig. 3 the "butterfly" multiplexing scheme might seem favorable because the X and Y contributions are farther separated in $S^{\bowtie}$ than they are in $S^{\square}$, the opposite is actually true: as illustrated by fig. 5, the demultiplexing process shifts the spectral contributions X and Y in different directions and whereas $X_Y^{\square}$ ends up centered around $\frac{f_s}{2}$, $X_Y^{\bowtie}$ is only separated by $\frac{f_s}{4}$ from the desired X at base band, effectively reducing the useful system bandwidth by a factor of two.

CONCLUSION

Multiplexing BPM processors suffer from $x{-}y$ crosstalk in addition to "normal" aliasing[3] as a consequence of a finite multiplexing rate. The crosstalk signal is shifted in frequency by an amount determined by the clock rate, the pickup geometry and scanning sequence.

REFERENCES

[1] R. Unbehauen, "Systemtheorie", Oldenbourg, Wien, 1993.

[2] W. Hess, "Digitale Filter", B.G. Teubner, Stuttgart, 1989.

[3] Although we assumed the motion to be band limited, in a real system the necessary filtering upstream of the RF detector is unrealizable. The multiplexed signal $s^{\square}$ could be filtered with a *band pass* around $\frac{f_s}{4}$ to eliminate crosstalk errors. Aliases from spectral components beyond the first Nyquist zone still constitute a problem, however.